Fuel 218 (2018) 357–365

Contents lists available at ScienceDirect

Fuel

journal homepage: www.elsevier.com/locate/fuel

Full Length Article

Thermally stable α-alumina supported ceria for coking resistance and oxidation of radical coke generated *in-situ*

Shilpa Mahamulkar[a], Kehua Yin[b], Micaela Taborga Claure[a], Robert J. Davis[b], Liwei Li[e], Hirokazu Shibata[c,1], Andrzej Malek[d], Christopher W. Jones[a,*], Pradeep K. Agrawal[a,*]

[a] School of Chemical & Biomolecular Engineering, Georgia Institute of Technology, Atlanta, GA 30332, USA
[b] Department of Chemical Engineering, University of Virginia, Charlottesville, VA 22904, USA
[c] Dow Olympic & Sports Solutions, Dow Chemical Japan, 2-2-24, Higashi Shinagawa, Shinagawa-ku, Tokyo 140-8617, Japan
[d] Hydrocarbons R&D, The Dow Chemical Company, Midland, MI 48674, USA
[e] Hydrocarbons R&D, The Dow Chemical Company, Freeport, TX 77541, USA

GRAPHICAL ABSTRACT

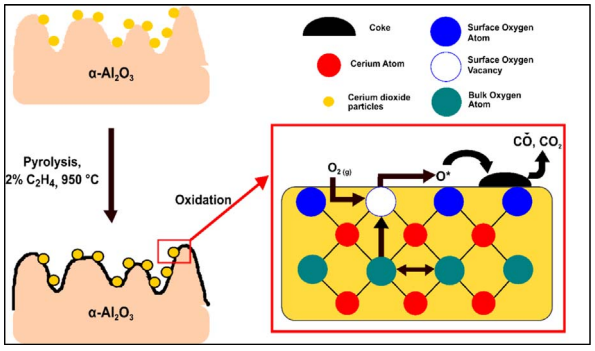

ARTICLE INFO

Keywords:
Coking
Coke – catalyst contact
Tight contact
Lattice oxygen
Decoking

ABSTRACT

A series of thermally stable α-alumina supported and unsupported ceria catalysts with varying composition is systematically investigated under realistic coke – catalyst contact conditions for the oxidation of *in-situ* generated coke during ethylene pyrolysis. These catalysts have been designed for use in high temperature applications of steam cracking. The textural and structural characterization of α-alumina supported ceria catalysts show the absence of solid oxide solutions, with the supported catalysts having distinct ceria domains on the alumina support. For comparison, two types of coke – catalyst contacting are explored: (i) tight contact by grinding industrial coke with catalyst and (ii) realistic *in-situ* contact, where coke is deposited on the catalytic support. During *in-situ* coke deposition, ceria-containing catalysts demonstrate resistance to coking as compared to the bare α-alumina support. Ceria and ceria – alumina composites also enabled coke oxidation at lower temperatures than the un-catalyzed coke oxidation. The presence of both Ce^{3+} and Ce^{4+} is confirmed by X-ray absorption near edge structure (XANES), consistent with the well-known redox capability of ceria catalysts. Kinetic studies revealed 50–80 mol% Ce as the best compositions for oxidation activity towards both industrial and *in-situ* coke. The catalytic activity correlates with the presence of reactive lattice oxygen atoms on ceria for both types of contact, indicating a similar mechanism of carbon oxidation under *in-situ* contact and tight contact conditions. A

* Corresponding authors.
E-mail addresses: cjones@gatech.edu (C.W. Jones), pradeep.agrawal@chbe.gatech.edu (P.K. Agrawal).
[1] Previously at Hydrocarbons R&D, Dow Benelux, The Netherlands.

https://doi.org/10.1016/j.fuel.2018.01.001
Received 12 October 2017; Received in revised form 26 November 2017; Accepted 1 January 2018
0016-2361/ © 2018 Elsevier Ltd. All rights reserved.

mechanism of reaction involving lattice oxygen of ceria is proposed for the oxidation of coke as well as for retardation of coke deposition on ceria domains.

1. Introduction

Radical carbonaceous deposits (coke) are generated at high temperatures during incomplete hydrocarbon combustion, for example, the coke formed in steam crackers during thermal decomposition of ethylene or propylene. Buildup of such deposits in reactors and on catalysts reduces the yield of desired products and requires frequent shutdowns or catalyst regeneration cycles, thereby increasing costs [1]. Hence, reduction in the accumulation of these deposits by fast oxidation is of significant interest in various chemical industries. In this work, catalytic materials that are resistant to coking and are active towards oxidation of carbon deposits are explored. These catalysts are active after high temperature treatment and can be used in high temperature applications such as steam cracking or pyrolysis reactions.

Steam cracking often involves thermal decomposition of ethane going to ethylene or propane going to propylene. The byproduct of this reaction is coke formation on the walls of the reactor. Coke deposited in the industrial steam crackers is typically combusted by passing air, other oxygen-containing gases, or mixtures thereof (e.g. steam and air) at high temperatures through the reactor in the regeneration mode. For instance, the steam cracker plant or process usually requires a shutdown for decoking every 20–60 days, depending on the type of feed used [2]. The physical structure and chemical nature of the carbon deposits depend on a number of factors, namely the operating temperature, pressure, residence time in the reactor and hydrocarbon feed composition. These aspects and others are summarized in an extensive review on different mechanisms of carbon formation and technologies used for reducing coke formation as well as for oxidation [3]. Coke deposition affects the production efficiency in a number of ways [4,1], such as increasing the pressure drop in the reactor [5], reducing the reactor volume, increasing the temperature of the steam cracker tube by affecting heat transfer from the tube to the gas, carburizing the steel, influencing flow in the reactor, and decreasing production capacity [6]. Hence, significant efforts have been focused towards the development of catalytic materials that can aid in the rapid and efficient oxidation of carbon deposits. In parallel, materials that can reduce the rate of deposition of carbon deposits are also sought-after.

Due to the nature of the solid-solid-gas reactions that occur for catalyzed carbon oxidation with an oxidizing gas, the contact between the carbon and the catalyst is very important. During the early studies of diesel soot (carbon) oxidation, Neeft et al. defined two types of contact between soot and catalyst – tight contact and loose contact [7]. The loose contact mixture was obtained by mixing the two materials with a spatula while the tight contact mixture was achieved by mixing the catalyst and soot in a mechanical mill for an extended time. Usually, the catalysts that are in tight contact with carbon are observed to have higher oxidation activity than those in loose contact conditions [8]. In fact, the ranking of catalysts for their oxidation activity can be different under loose and tight contact conditions [9]. To achieve reproducible results and effectively screen catalysts for carbon oxidation activity, most researchers perform experiments with samples under tight contact conditions. In this paper, catalytic activity under another type of coke – catalysts contact, *in-situ* coke – catalyst contact, where coke is directly deposited on the catalyst, has been measured. This is a near exact representation of how carbon and catalyst would come in contact in an industrial setting. The *in-situ* coke deposition method has been described in the previous study [10].

Over the last decades, cerium oxide and mixtures of cerium-containing oxides have been found to be effective for a number of oxidative catalytic processes. An important characteristic of ceria is its redox capability under both oxidizing and reducing conditions. Cerium based oxides have been used in the three-way catalytic converter for elimination of CO, hydrocarbons, and NO_x in engine exhaust due to their excellent oxygen storage capacity. Their highly active surface crystal facets and redox behavior allow cycling between Ce^{3+} and Ce^{4+} states with the formation and elimination of oxygen defects [11,12]. Such materials have also received wide attention for diesel soot oxidation. The soot formed in diesel engines is due to the incomplete combustion of the fuel and has a similar mechanism of formation as the steam cracker coke. Hence, use of similar catalytic materials that have been used for soot oxidation was the first choice. Oxygen vacancy defects are known to be one of the most reactive sites on metal oxides [13,14]. The redox chemistry of ceria can be written as:

$$2CeO_2(s) \rightarrow 2CeO_{2-y}(s) + yO_2(g) \quad (1)$$

where, CeO_{2-y} is a non-stoichiometric phase. The oxygen storage capacity of ceria can be enhanced by doping it with other rare earth elements [15]. Ceria catalysts are promising candidates for applications like soot oxidation [11,16–20], the water gas shift reaction [15], CO oxidation [21], and in solid oxide fuel cells [22–24].

Doping of ceria with zirconium has been observed to increase the oxygen storage capacity of ceria and enhance catalytic activity towards oxidation of soot [11,25–27]. Most of the soot oxidation studies involving ceria work with temperatures below 800 °C, above which compositional changes might take place affecting the properties of the catalyst [26]. However, steam cracker units operate at temperatures around 1000 °C and hence, thermal stability of the catalytic materials is of high importance. As a consequence, any support material used should be inert, stable under operating conditions and low cost. In steam cracking reactions, the wall of the reactor is made of Ni, Fe, Cr alloys that cause catalytic coking, leading to formation of filamentous coke. This coke can act to deteriorate the strength of the reactor by carburization of the alloy. To create a barrier between the hydrocarbons and the metallic species on the wall reactor, an intermediate layer of α-alumina is proposed. α-Alumina is the most thermodynamically stable phase of alumina, has very low surface area but high corrosion resistance, which makes it an appropriate candidate for high temperature applications. An active layer of ceria on top of the α-alumina layer is considered for its catalytic activity towards coke oxidation. A detailed study on the coatings of the same catalytic system on a metallic substrate will be discussed in the later studies [28]. In these studies, the presence of α-alumina as a barrier has been found to be critical for sustaining the catalytic activity of the ceria. To understand the effect of the α-alumina support on the activity of the ceria catalyst, the present studies were performed and were compared with the bulk ceria catalyst.

In this work, we sought to design catalysts that are active for oxidation of coke formed during steam cracking. Accordingly, the objective of this study was to develop catalytic materials that aid coke oxidation and minimize coke deposition in high temperature applications and investigate the properties responsible for their activity. Ceria dispersed on a commercial α-alumina support at various loadings was used to explore coke deposition as well as oxidation of coke. Two types of coke – catalyst contact were examined, (i) traditional tight contact and (ii) *in-situ* contact. The alumina-supported cerium oxides were also characterized by various analytical techniques, allowing for their oxidation performance to be correlated with their composition and structural properties.

2. Materials and methods

2.1. Catalyst synthesis

Ceria loaded α-alumina materials were prepared by a wetness impregnation method using cerium nitrate hexahydrate ($Ce(NO_3)_3{\cdot}6H_2O$, Sigma Aldrich) as the cerium precursor and α-alumina as the support (Sigma Aldrich, corundum, -100 mesh, 99%). The mixture was dried at 110 °C overnight and calcined at 1100 °C for 8 h after heating at a rate of 1 °C/min in air. The synthesized catalysts are denoted as x-CeO_2-Al_2O_3, where x denotes Ce/(Ce + Al) atomic ratio in the catalyst sample. An industrial coke sample was obtained from The Dow Chemical Company.

2.2. Catalyst characterization

Catalyst samples were characterized by nitrogen physisorption, X-ray diffraction, Raman spectroscopy, UV–Vis spectroscopy, and temperature programmed reduction. Nitrogen physisorption isotherms were collected at −196 °C using a Micromeritics Tristar II. The samples were heated to 200 °C under vacuum for 10 h prior to the analysis. The data obtained were used to calculate surface areas for the various powders. The powders were characterized by X-ray diffraction (XRD) using Cu K α radiation. The instrument was operated at 40 mA and samples were packed into a horizontally mounted sample holder. The crystallite sizes were estimated using the Scherrer equation. A Witec confocal Raman microscope (Alpha 300R) was used to obtain Raman spectra for the fresh and coked catalysts with an Ar^+ ion laser (λ = 513.998 nm) using a 2 mW excitation source intensity and 1800 grating with $< 0.9\,cm^{-1}$ pixel resolution. A magnification of 50× was used. A dense sample layer of about 1 mm thickness was pressed onto a cover slip with the help of a spatula. This coverslip was then placed on the microscope sample holder. A white light source was used to focus on the surface of the sample. After focusing on a spot, the sample was exposed to the laser beam and the Raman spectra were recorded at ambient temperature. First order Raman spectra were de-convoluted using the peak analyzer function of the OriginPro 8.5 software.

X-ray absorption spectroscopy (XAS) was performed at beamline X18B of the National Synchrotron Light Source (NSLS), Brookhaven National Laboratory. The X-ray absorption near edge structure (XANES) was derived from spectra collected in the transmission mode at the Ce L_{III} edge (5723 eV). The Ce L_{III} edge spectra were measured at room temperature in air. The samples were prepared by spreading a thin layer of material on pieces of transparent tape. CeO_2, obtained from Sigma Aldrich, was used as a standard. Two scans from 5,573 to 6,187 eV were collected for each sample. The XAS data were then processed with Athena software for background removal, and edge-step normalization.

The ceria lattice oxygen species available for oxidation reactions at different conditions were measured by temperature programmed reduction (TPR) experiments on a Micromeritics AutoChem 2920. The samples were pretreated at 150 °C in He for 1 h to remove volatile species. Approximately 40–50 mg of the sample was heated at a constant rate (5 °C/min) from room temperature to 900 °C in 10% hydrogen in argon (30 mL/min), in a U-shaped quartz tube. The water produced was removed by passing the effluent gas through a cold trap (a mixture of acetone and liquid nitrogen). Hydrogen consumption was monitored by a thermal conductivity detector. For quantitative analysis, the instrument was calibrated with the reduction of Ag_2O. UV–Vis spectroscopy measurements were performed in the wavelength range of 200–800 nm using a Cary UV–Vis NIR spectrophotometer. The instrument was calibrated using $BaSO_4$ as the standard.

2.3. Coke – catalyst contact

2.3.1. In-situ coke – catalyst contact

A customized thermogravimetric analyzer (TGA, Netzsch, STA449F3 Jupiter®) was used for *in-situ* generation of radical coke (coke formed in gas phase) and to study coke oxidation. This TGA could be operated with reactive gases like hydrocarbons at high temperatures. For safety reasons, flammable gas concentrations were kept below their flammability limits in the TGA. In these experiments, 2 mol% of ethylene was used. The internal components of this TGA were designed to work efficiently in the presence of corrosive atmospheres. The measurement head, made of alumina, was stable at high temperatures and resistant to corrosive gases.

For *in-situ* coke deposition, the TGA furnace was heated to the desired temperature in helium flow. Once the desired temperature was reached, 2 mol% ethylene in helium was introduced into the system for 1 h. After 1 h, the ethylene flow was stopped and the furnace was allowed to cool while under helium flow. The coking rate and the amount of coke deposited were measured by the TGA. Coke deposited on the measurement head was removed completely prior to oxidation of the coked catalysts, by temperature programmed oxidation in air up to 900 °C after removal of the coked catalyst sample. The coke thus formed was used as a model coke sample to represent the steam cracking of ethane.

2.3.2. Tight contact

For tight contact experiments, an industrial coke sample obtained from a steam cracker from The Dow Chemical Company was used. A small amount of industrial coke and catalyst in the ratio 1:9 were ground in a mortar and pestle for 45 min to achieve tight contact conditions.

2.4. Catalytic activity

2.4.1. Temperature programmed oxidation

Temperature programmed oxidation (TPO) experiments were also performed on the Netzsch TGA. The TGA was used to determine the reactivity of the coke deposited on various catalyst materials. For these measurements, 15 mg of the coke – catalyst mixture was placed in an alumina crucible. The temperature was raised from room temperature to 950 °C at a rate of 10 °C/min in the presence of air (100 mL/min). The rate of mass loss was used to compare the activity of catalysts for both the industrial and *in-situ* coke samples.

2.4.2. Isothermal oxidation

Isothermal oxidation was carried out on the Netzsch TGA by heating the coke – catalyst sample to the desired temperature under helium flow. Once the desired temperature was reached, air was introduced into the furnace. Rate constants were obtained by fitting the mass loss data to a first order rate equation. The data from 0 to 50% conversion were used to calculate the rate constants. Isothermal studies were also performed in the absence of any oxidizing agent under helium flow to establish a baseline or to study the effect of lattice oxygen species present in ceria.

2.4.3. Isothermal reduction of catalysts

Isothermal reduction of catalysts was carried out at the reaction temperature (950 °C) to determine the amount of oxygen released during the pyrolysis reaction where hydrogen is produced. The TGA furnace was heated to the desired reaction temperature in nitrogen flow. Once the desired temperature was reached, 1.5 mol% hydrogen in nitrogen was introduced into the system for 1 h. After 1 h, the hydrogen flow was stopped and the furnace was allowed to cool while under helium flow.

3. Results and discussion

3.1. Catalyst characterization

Fig. 1 compares the XRD patterns for α-alumina supported ceria catalysts along with unsupported ceria and the α-alumina support. The α-alumina peaks (25°, 35°, 37°, 43°, 52°, 66°, 68°, 77°) do not disappear in the catalysts but the relative intensity of these peaks decreases in comparison to the ceria diffraction peaks. This decrease could be attributed to the increasing amounts of ceria in the catalyst and also the increasing particle size of ceria, which causes sharp peaks. The low resolution of the peaks seen in the graph is due to the normalization of the diffraction pattern with respect to the dominant ceria peak at ~28°. The α-alumina peaks are visible in a large size plot of the diffraction patterns of the various catalysts, as shown in Figs. S1 and S2. All α-alumina supported ceria composites showed distinct ceria peaks. Diffraction peaks corresponding to fluorite structure of CeO_2 (28.6°, 33.3°, 47.5°, 56.4°) [29] were well defined in the diffractograms of the composites. Peak broadening was used to determine crystallite size based on the (1 1 1) plane of ceria. These sizes are in the range of 30–60 nm, as summarized in Table 1.

The surface areas of the various materials are summarized in Table 1. Since, the surface areas are very low, around 1.5–2 g of the catalysts were used for physisorption analysis. Catalysts with 20 and 50 mol% Ce had slightly higher surface areas than bare α-alumina. Higher ceria loadings of 80 mol% reduced the surface area. From the physisorption experiments, it was observed that the catalytic materials were highly non-porous in nature. This is attributed to the non–porous nature of the commercial α-alumina support that was used, as well as the high calcination temperature. Both aspects make these catalysts thermally stable so they can be used in high temperature applications. Unsupported ceria showed higher surface area than the supported ceria samples, but it had a similar non-porous nature.

Fig. 2 shows that XANES spectra for bulk ceria and α-alumina supported ceria are similar to the reference ceria sample obtained commercially. Two major peaks at 5731 eV (A) and 5738 eV (B) are present in all the catalysts' spectra. These peaks have been associated with the +4 oxidation state of Ce [30]. The difference in the intensity of the peaks for various catalysts is related to the crystallite size of the catalysts. The larger the crystallite size of the materials, the higher the intensity of the A and B peaks, which is also consistent with the sizes obtained from XRD analysis (Table 1). A minor peak (C) at 5727 eV indicates the presence of Ce species in the + 3 oxidation state in the supported and unsupported ceria catalysts. Peak D is a part of the pre-edge region and is located at 5720 eV. Peak D arises due to the electronic transitions at the bottom of the conduction band. The presence of the +3 and +4 oxidation states of Ce is consistent with the well-known redox nature of the catalysts, and also demonstrates that chemical nature of the unsupported ceria and ceria supported on alumina is the same. Hence, there are no interactions between ceria and alumina species in the supported materials that would change the electronic structure of the ceria.

Fig. 3 shows Raman spectra of the supported and unsupported ceria catalysts. A peak at ~470 cm^{-1}, characteristic of CeO_2 (F_g mode), was observed for all samples [31]. This indicates the presence of characteristic CeO_2 domains in the catalysts. The spectral features at 250, 268, 288, 383, 558 cm^{-1} have been observed on ceria dispersed on γ-alumina investigated by Shyu et al. [31] and have been associated with a $CeAlO_3$ species. The absence of these peaks in the spectra for the α-alumina supported ceria catalysts in Fig. 3, denotes the absence of any intermixing between Ce and Al species. Thus, results from XANES and Raman spectroscopy demonstrate the presence of independent CeO_2 domains on the surface of α-alumina, without any intermixing with the alumina species, for all the α-alumina supported ceria samples.

Nano-crystallites in a material can escape XRD detection due to their small crystal size. In such cases, UV absorption can be used to detect their presence. Fig. S4 shows the UV spectra of both the supported and unsupported ceria catalysts. An absorption band at around 370–380 nm was observed for all the catalysts and has been attributed to inter-band transitions, which is in agreement with values in the literature for transmission on single ceria crystals [32]. This observation is again an indication of a lack of significant interactions between the ceria and alumina species in the α-alumina supported ceria catalysts. The detailed analysis of absorption edge wavelengths is shown in Fig. S5 and Table S2. Absorbance at lower wavelengths ≤375 nm indicated the presence of smaller crystallites (≤4 nm) that were not detected by XRD [32].

TPR experiments of the α-alumina supported ceria materials and unsupported ceria were performed to analyze the reduction properties of the catalysts. Two major peaks were observed for both the unsupported and supported ceria (Fig. S6), referred to here as the low temperature and the high temperature peak, respectively, whose values are shown in Fig. 4. This is consistent with the reduction profiles for ceria reported by others in the literature [29,33]. Unsupported ceria has higher temperature values for both the peaks than the α-alumina supported ceria (Fig. 4). The presence of two peaks depicts the step-wise reduction of CeO_2. The low temperature peak has been typically associated with the removal of surface lattice oxygens of CeO_2 [29,34,35]. The higher temperature peak is then associated with the progressive reduction of the bulk CeO_2. However, the transition between the surface and bulk cerium atoms is more gradual than sudden. Hence, there can be an overlap of surface and bulk reduction that happens at intermediate temperatures. Bulk ceria, when reduced, leads to formation of Ce_2O_3 [29]. Visually this compound appears bluish black in color. All samples after the TPR runs turned bluish black, indicating the reduction of bulk ceria. The total hydrogen consumption of these catalysts during reduction is included in Table S4.

3.2. Coking resistance of α-alumina supported ceria catalysts

Metallic and acidic catalysts are well known to catalyze coke formation [36,37]. Inhibition of coke deposition requires the catalysts to also be coke–resistant. To demonstrate the coke resistance abilities of the ceria catalysts, *in-situ* coke deposition was performed in the TGA.

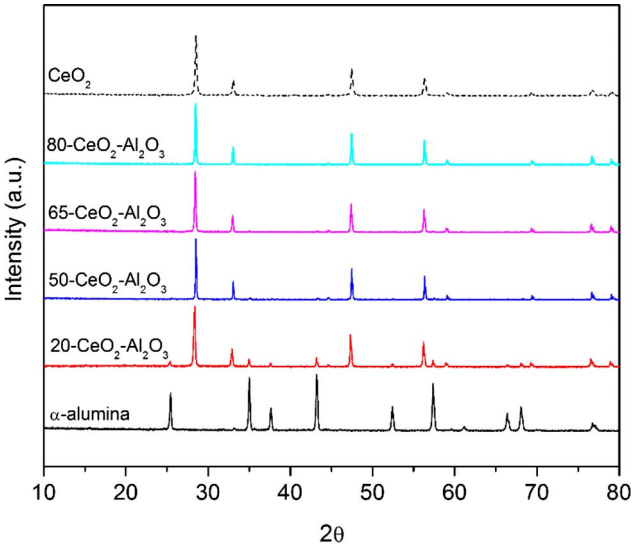

Fig. 1. XRD patterns of α-alumina, unsupported ceria and ceria-alumina composites with different ceria loading.

Table 1
Crystallite sizes of the ceria (111) plane at θ ~ 28° and textural properties of catalysts.

Sample	XRD crystallite size 111 peak (nm)	Surface area (m^2/g)
α-alumina	–	1.5
CeO_2	42	7.0
20-CeO_2-Al_2O_3	32	1.9
50-CeO_2-Al_2O_3	57	2.1
65-CeO_2-Al_2O_3	47	1.9
80-CeO_2-Al_2O_3	53	1.0

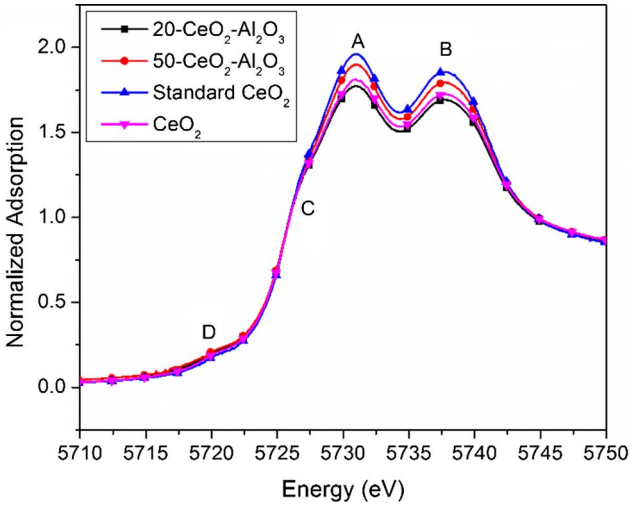

Fig. 2. Ce L_{III}-edge XANES spectra of unsupported and supported ceria.

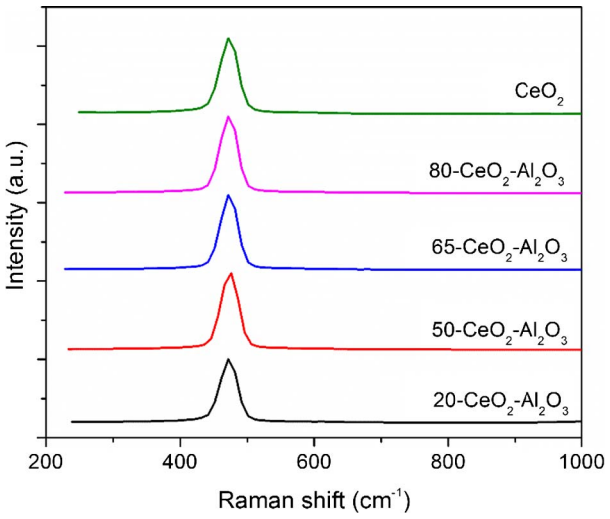

Fig. 3. Raman spectra of the ceria catalysts; 514 nm, 2 mW.

Coke deposition on α-alumina (0 mol% Ce) was used as a reference case. In the previous study, it was demonstrated that *in-situ* coke deposition was independent of the catalytic support and that radical coke was deposited on the supports [10]. Here, the support materials of equal surface areas were exposed to 2% ethylene in helium at 950 °C for 1 h. The amount of coke deposited on these supports is shown in Fig. 5. The maximum amount of coke deposition was observed on the reference α-alumina support. All the ceria catalysts showed lower amounts of coke deposition. This observation can be attributed to the ability of ceria to provide oxygen to the deposited coke precursors for *in-situ* oxidation of coke species, slowing coke deposition to a degree. The bulk ceria material had the least amount of coke deposited on its surface. To calculate the amount of oxygen that may be labile and thus

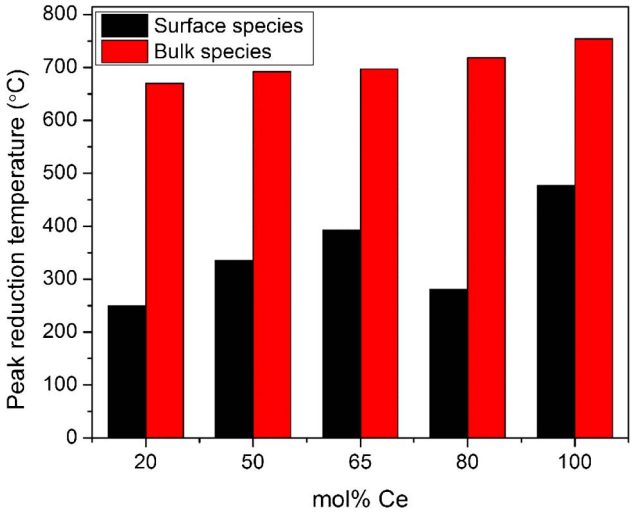

Fig. 4. Peak reduction temperature of unsupported and supported ceria materials from TPR analysis.

given up by the ceria catalyst in the presence of the reducing hydrogen produced during pyrolysis of ethylene, the catalysts went through the same thermal treatment as the pyrolysis reaction in the presence of 1.5 vol% hydrogen alone. Table S2 shows the values for isothermal reduction of the catalysts and the amount of coke deposition observed on them. For the highest (20 mol% Ce) and lowest (CeO_2) amounts of coke deposited, there is a clear correlation with the amount of hydrogen consumed by the catalysts, which correlates with the amount of oxygen released by the catalyst under pyrolysis conditions. For the other catalysts, the resolution between the values for hydrogen consumed is quite low and hence comparison is difficult. Further studies are required that can capture the redox nature of these catalysts at high temperatures with improved accuracy.

Raman analysis is an effective way to determine the type of carbon species in the coked samples. Deconvolution of the Raman peaks reveals interesting information on the amorphous carbon content in the coke samples. Raman spectra of *in-situ* coke was deconvoluted into five peaks (G, D_1, D_2, D_3, D_4), where D_3 is the amorphous carbon peak observed at 1500 cm^{-1} [38]. Sadezky et al. found that fitting the G, D_1, D_2, D_4 peaks as Gaussian and the D_3 peak as Lorentzian gave the best fit for the spectra [38]. Similar deconvolution analysis (Fig. S3) was used for obtaining Raman parameters for the different coked samples. The

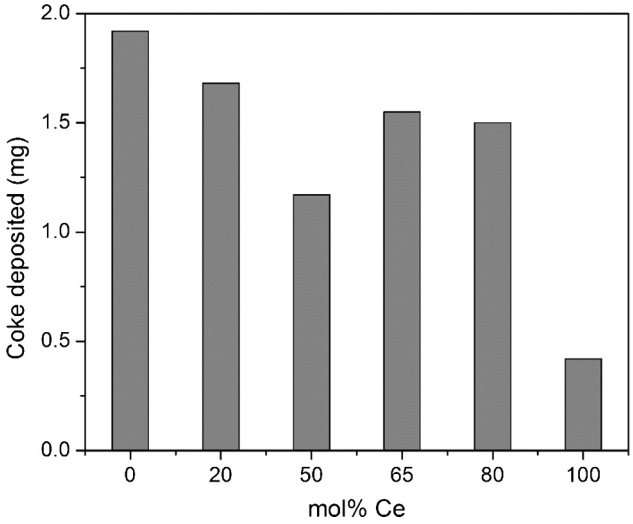

Fig. 5. Comparison of coking resistance of the supported ceria catalysts with unsupported ceria and the α-alumina support.

heterogeneity of the coke samples was studied by measuring the Raman spectra at different spots on the sample. The relative intensity of the amorphous carbon is given by the following equation [39]:

$$Relative\ intensity\ of\ D_3 = \frac{I_{D3}}{I_{D3} + I_G + I_{D2}} \quad (2)$$

Fig. 6 shows the amount of amorphous carbon in the coke deposited on the ceria catalysts in comparison with the bare α-alumina support. Coke formed on the α-alumina had lower amorphous content than the coke formed on the ceria catalysts. These data demonstrate that ceria catalysts not only reduced the amount of coke deposition relative to the α-alumina, but the deposited carbon also formed less hard coke under the conditions used. This observation may be attributed to the ability of ceria to oxidize coke precursors as they become deposited on the surface of the powder catalyst. Ceria catalysts thus appeared to not only reduce the amount of coke deposited but also to reduce the hardness of the deposited coke.

3.3. Temperature programmed oxidation studies of coke using α-alumina supported ceria

To investigate the activity of the ceria catalysts towards oxidation of coke, temperature programmed oxidation studies were performed under two coke – catalyst contact conditions. For the tight contact conditions (Fig. 7a), uncatalyzed (0 mol% Ce) industrial coke oxidized at a very high T_{50} (temperature at which 50% of the coke was oxidized) value of ~650 °C. This value reduced significantly (by ~100 °C) in the presence of the ceria catalysts. All the ceria catalysts reduced this T_{50} value to a comparable degree, as shown in Fig. 7a. For *in-situ* deposited coke, Fig. 7b demonstrates that the coke deposited on α-alumina (0 mol % Ce) had the highest T_{50} value (~550 °C) and hence, was the most difficult to oxidize. This observation is likely related to the hardness of the coke, as seen in Section 3.2, and the low catalytic activity of α-alumina towards coke oxidation. The presence of ceria in the catalyst reduced the T_{50} value by ~150 °C for all ceria-containing materials (Fig. 7b). Oxidation of coke on α-alumina supported ceria and bulk ceria catalysts showed very little variability in the T_{50} value.

3.4. Catalytic activity of coke combustion over ceria-alumina

To measure the kinetics of the catalytic oxidation of coke, isothermal experiments were performed on the tight contact coke – catalyst mixtures (Fig. 8) and the *in-situ* coked catalysts (Fig. 9). The lower temperatures were chosen for isothermal studies such that non-catalytic oxidation of coke was kept relatively low. As shown in Fig. 8, at 450 °C and in the presence of a ceria-containing catalyst, the catalytic activity was improved compared to experiments using the ceria-free alumina support. However, the differences in the kinetic constants for the catalysts with different ceria content were minimal. At an increased temperature of 500 °C, the catalytic effect was significantly enhanced. The catalytic activity of the 50-CeO_2-Al_2O_3 material was five times that of the uncatalyzed oxidation. Unsupported ceria showed the lowest catalytic activity at both temperatures for the tight contact conditions. The 20-CeO_2-Al_2O_3 material showed increased catalytic activity as compared to the un-catalyzed oxidation. As the mol% Ce was increased from zero to 50%, the catalytic activity increased. However, after 50 mol% Ce loading, the activity remained steady without any further improvement. This behavior was observed for both the coke-catalyst contact conditions, indicating the similarity of *in-situ* and tight contact conditions, with both exhibiting intimate contact between the coke and catalyst particles. As shown in Fig. 9, coke deposited on the α-alumina support did not oxidize at all, which is likely related to the lack of redox activity of the α-alumina. The *in-situ* coke deposited was more amorphous than the industrial coke sample and hence, the temperature chosen for kinetic studies was lower for the *in-situ* coke. As a result, the reaction rates cannot be compared for the two temperature ranges, as the nature of the carbon species used was different [3].

Similar isothermal experiments were carried out in the absence of oxidizing gas under helium flow at 450 °C. Industrial coke did not show any weight loss in the absence of a catalyst as well as the oxidizing agent. As expected, the reaction progressed significantly slower as compared to studies where air was present. In the presence of a catalyst, the weight loss followed a zero order rate model. This observation demonstrates the ability of the ceria catalyst to provide oxygen to the carbon species in the absence of gaseous oxygen. No weight loss occurred when a similar heat treatment was given to bare catalysts without coke, indicating the weight loss observed during isothermal oxidation experiments was entirely due to loss of carbon species. The rate constants for the gasification in inert were calculated for the 0–10% conversion region of the industrial coke for the uncatalyzed (no catalyst) as well as catalyzed reactions, as shown in Table 2. The theoretical total surface oxygen species that are available on the ceria catalysts were calculated based on the average exposure of 111, 110 and 100 crystal planes of ceria, assuming Al atoms were not reduced and one out of four Ce atoms was reduced [40]. As the theoretical amount of surface oxygens in the sample increased, the rate of gasification of carbon under inert conditions increased too, implying the importance of surface oxygen release by ceria leading to carbon oxidation. This theoretical value calculates only the contribution from surface oxygen species as opposed to bulk oxygen species, which are active at the high temperature of 950 °C used for measuring the hydrogen consumption in Table S1. Hence the order of magnitude observed for values in Table 2 and Table S1 cannot be directly compared.

3.5. Relating catalytic activity to ceria lattice oxygen content

Temperature programmed reduction curves showed that the α-alumina supported ceria samples had a lower overall reduction temperature than bulk ceria. Surface reduction of the ceria, associated with the low temperature peak, also improved when ceria was dispersed over α-alumina. The amount of lattice oxygen available for reduction up to a specific temperature was calculated from the TPR data, as discussed above. The majority likely consisted of surface lattice oxygen species due to the low temperatures used for coke oxidation. However, the possibility of contribution from bulk lattice oxygens cannot be neglected. A good correlation was found between the available ceria lattice oxygen species and the kinetic rate constants calculated from the isothermal oxidation data. Interestingly, this observation was obtained for both the tight contact (Fig. 10) and *in-situ* coke – catalyst (Fig. 11)

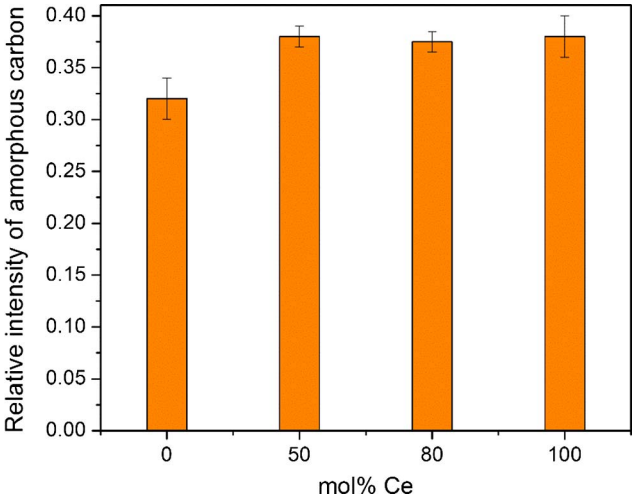

Fig. 6. Deconvolution of Raman spectra of coked catalyst samples comparing the relative amorphous nature of the coke deposited *in-situ* on the various materials.

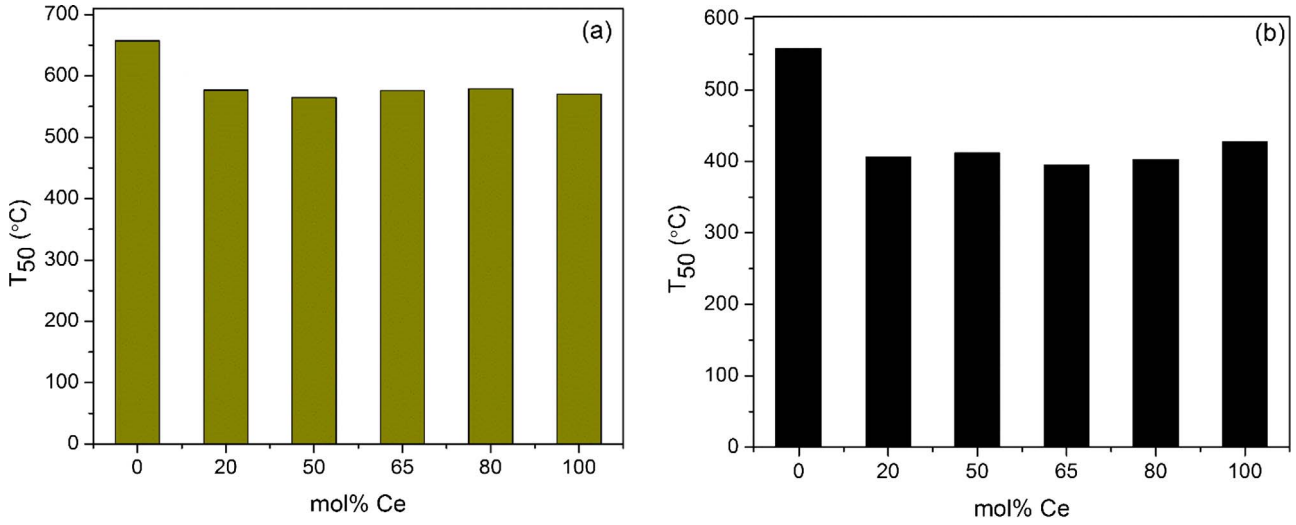

Fig. 7. T_{50} values for oxidation of (a) industrial coke (b) *in-situ* coke.

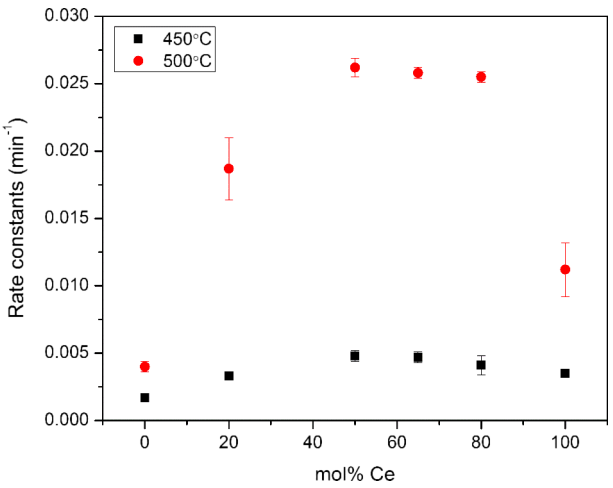

Fig. 8. Kinetic studies for oxidation in tight coke-catalyst conditions with the industrial coke sample at 450 °C and 500 °C in air.

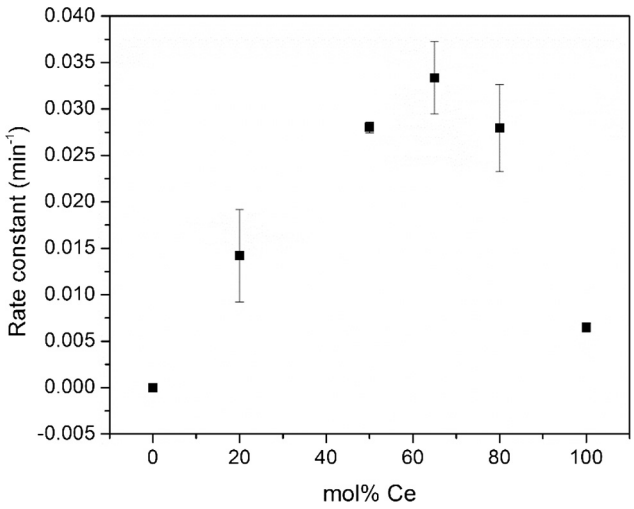

Fig. 9. Kinetic studies for oxidation using in-situ coke-catalyst contact conditions at 350 °C in air.

Table 2
Rate constants for gasification of coke in inert gas environment.

Catalyst	Rate constant, industrial coke, inert gas, ($g_{carbon}\,min^{-1}$), 450 °C	Theoretical surface oxygens available, μmol/g
–	0.0000	–
20-CeO_2-Al_2O_3	0.0004	2.1
50-CeO_2-Al_2O_3	0.0008	5.7
65-CeO_2-Al_2O_3	0.0007	6.7
80-CeO_2-Al_2O_3	0.0006	4.4
CeO_2	0.0009	37.5

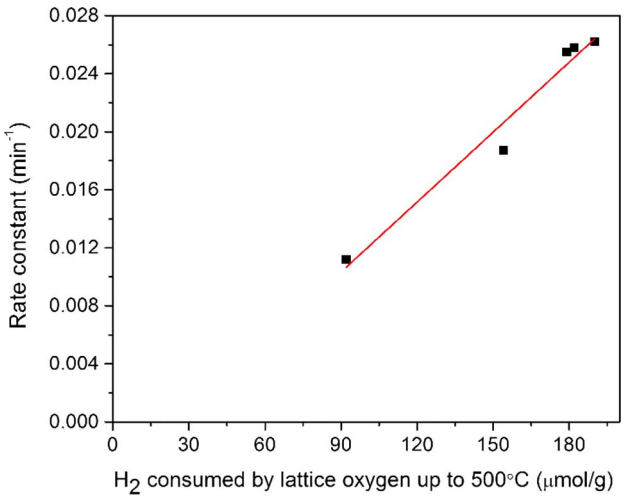

Fig. 10. Relating the reaction rate constant to ceria lattice oxygen availability for tight coke-catalyst contact.

contacting conditions. This strengthens the previous observation that *in-situ* coke – catalyst contact showed similar oxidation behavior as tight contact conditions [10].

3.6. Proposed mechanism of coke oxidation over α-alumina supported ceria

In the previous section, it was demonstrated that the lattice oxygens from ceria were responsible for the observed enhanced activity towards

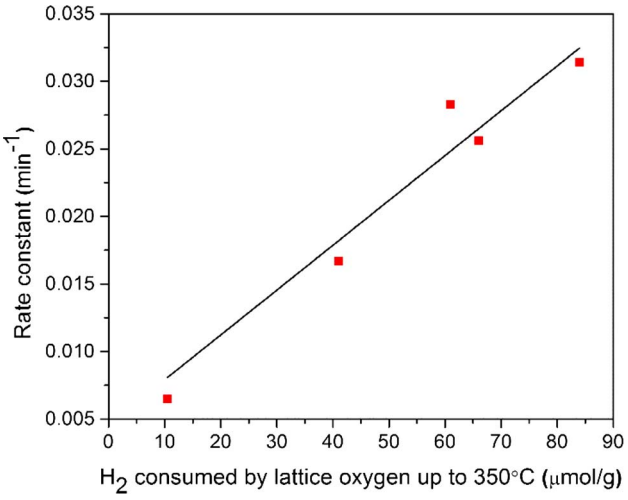

Fig. 11. Relating the reaction rate constant to ceria lattice oxygen availability for in-situ coke – catalyst contact.

oxidation of coke. Based on this observation, a mechanism of coke oxidation is proposed. Fig. 12 shows a schematic of *in-situ* coke formation and the hypothesized mechanism of coke oxidation using the ceria catalysts. During pyrolysis, coke was formed on both ceria and α-alumina. Since it has been shown that individual ceria domains of varied crystallite sizes exist on the surface of the α-alumina support, the schematic shows only ceria as the catalytic surface. As seen from the TPR results, ceria has two types of lattice oxygens available for reduction, namely surface oxygens and bulk oxygens. Based on the temperature range of coke oxidation, the contribution of bulk oxygen changes and as expected, it increases with temperature. In the proposed mechanism, under the conditions used here, primarily surface lattice oxygen are thought to participate in the oxidation reactivity. It is proposed that surface lattice oxygen from ceria forms an active species (O∗) at the coke – ceria interface. This active species reacts with coke to form volatile carbon oxides. Gaseous oxygen fills the oxygen vacancy formed by the loss of oxygen. Simultaneously, there is increased mobility in the bulk of ceria and diffusion of bulk lattice oxygens to the surface that can fill up the oxygen vacancies. This mechanism has been proposed for ceria – zirconia materials for soot oxidation [25] and CO oxidation [41], ceria [13], ceria – lanthana [33,35], copper – ceria for CO oxidation [42], etc. previously.

4. Conclusions

Thermally stable ceria supported on α-alumina and unsupported ceria appeared to be resistant to coking and useful in the oxidation of coke deposits under realistic *in-situ* contact conditions. Using α-alumina as the support renders these catalysts suitable for high temperature application of steam cracking for use up to ~1000 °C. Surface characterization of catalysts by XANES and Raman spectroscopy revealed the presence of independent CeO_2 domains with no significant electronic interactions with the alumina support. XRD gave evidence of large crystallites and smaller crystallites were inferred to exist based on UV–Vis spectroscopy. Two types of coke – catalyst contact were investigated for coke oxidation, tight contact between the catalysts and industrial coke and *in-situ* contact where carbon was deposited directly on the catalysts. Ceria catalysts were observed to show coking resistance when compared to bare α-alumina support during *in-situ* coking. This ability was qualitatively related to the ability of the ceria catalyst to release oxygen in a reducing environment. The oxidation performance was probed by temperature programmed and isothermal oxidation studies. In both coke-catalyst contact conditions, α-alumina supported ceria materials were observed to have better oxidation capability towards the coke deposits than bulk ceria. The kinetics of coke oxidation were correlated to the availability of ceria lattice oxygen, which was obtained from temperature programmed reduction studies. The similarity observed for the behavior of coke oxidation activity in these two contact conditions indicates that *in-situ* coke – catalyst contact mimics tight contact conditions. A mechanism involving lattice active adsorbed oxygen species causing oxidation of coke particles was proposed.

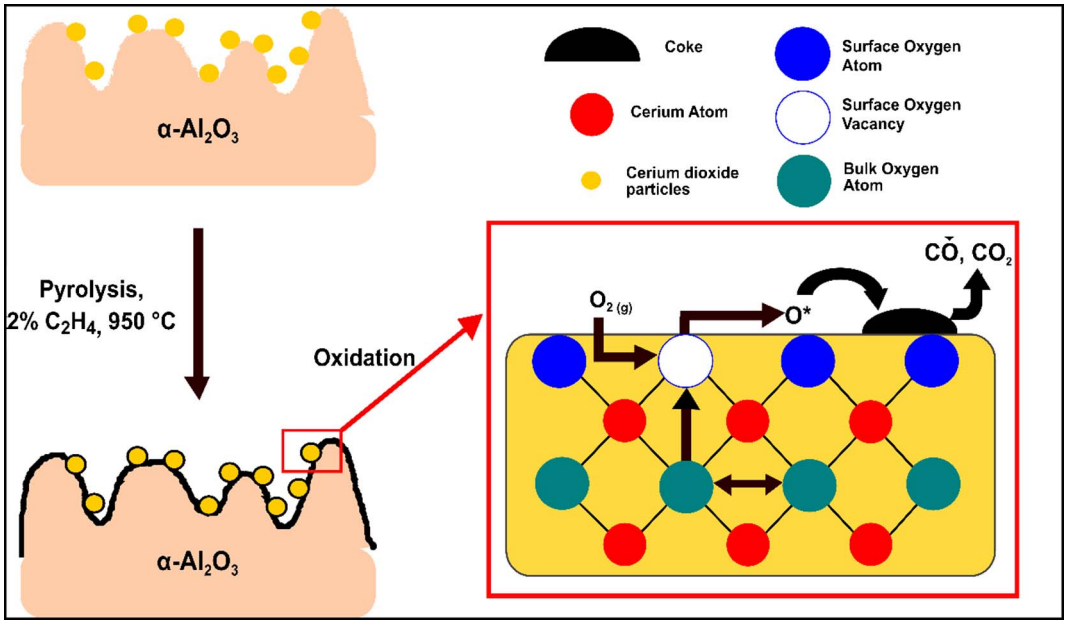

Fig. 12. Schematic representation of the mechanism of coke oxidation on ceria and supported ceria catalysts.

Acknowledgements

The financial support for this work was provided by The Dow Chemical Company. Use of the National Synchrotron Light Source, Brookhaven National Laboratory, was supported by the U.S. Department of Energy, Office of Science, Office of Basic Energy Sciences, under Contract No. DE-AC02-98CH10886. The authors also wish to express special thanks to the assistance received from X-18B beamline personnel, Dr. Syed Khalid and Dr. Nebojsa Marinkovic.

Appendix A. Supplementary data

Supplementary data associated with this article can be found, in the online version, at http://dx.doi.org/10.1016/j.fuel.2018.01.001.

References

[1] Cai H, Krzywicki A, Oballa MC. Coke formation in steam crackers for ethylene production. Chem Eng Process Process Intensif 2002;41:199–214. http://dx.doi.org/10.1016/S0255-2701(01)00135-0.
[2] Sundaram KM, Van Damme PS, Froment GF. Coke deposition in the thermal cracking of ethane. AIChE J 1981;27:946–51. http://dx.doi.org/10.1002/aic.690270610.
[3] Mahamulkar S, Yin K, Agrawal PK, Davis RJ, Jones CW, Malek A, et al. Formation and oxidation/gasification of carbonaceous deposits: a review. Ind Eng Chem Res 2016;55:9760–818. http://dx.doi.org/10.1021/acs.iecr.6b02220.
[4] Chan KYG, Inal F, Senkan S. Suppression of coke formation in the steam cracking of alkanes : ethane and propane. Ind Eng Chem Res 1998;37:901–7.
[5] Shah Y, Stuart E, Sheth K. Coke formation during thermal cracking of n-octane. Ind Eng Chem Process Des Dev 1976;15:518–23.
[6] Niaei A, Salari D, Towfighi J, Chamandeh A, Nabavi R. Aluminized steel and zinc coating for reduction of coke formation in thermal cracking of Naphtha. Int J Chem React Eng 2008;6:1–11.
[7] Neeft JPA, Makkee M, Moulijn JA. Catalysts for the oxidation of soot from diesel exhaust gases. I. An exploratory study. Appl Catal B Environ 1996;8:57–78. http://dx.doi.org/10.1016/0926-3373(95)00057-7.
[8] Neeft JPA, Makkee M, Moulijn JA. Catalytic oxidation of carbon black – I. Activity of catalysts and classification of oxidation profiles. Fuel 1998;77:111–9.
[9] Shimokawa H, Kurihara Y, Kusaba H, Einaga H, Teraoka Y. Comparison of catalytic performance of Ag- and K-based catalysts for diesel soot combustion. Catal Today 2012;185:99–103. http://dx.doi.org/10.1016/j.cattod.2011.10.030.
[10] Mahamulkar S, Yin K, Davis RJ, Shibata H, Malek A, Jones CW, et al. In situ generation of radical coke and the role of coke-catalyst contact on coke oxidation. Ind Eng Chem Res 2016;55:5271–8. http://dx.doi.org/10.1021/acs.iecr.6b00556.
[11] Machida M, Murata Y, Kishikawa K, Zhang D, Ikeue K. On the reasons for high activity of CeO_2 catalyst for soot oxidation. Chem Mater 2008;20:4489–94.
[12] Yao YU. Ceria in automotive exhaust catalysts. J Catal 1984;86:254–65.
[13] Campbell CT, Peden CHF. Oxygen vacancies and catalysis on ceria surfaces. Science (80-.) 2005;309:713–4. http://dx.doi.org/10.1126/science.1113955.
[14] Trovarelli A. Catalytic properties of ceria and CeO_2 – containing materials. Catal Rev Sci Eng 1996;38:440–509.
[15] Gorte RJ. Ceria in catalysis: from automotive applications to the water-gas shift reaction. AIChE J 2010;56:1126–35. http://dx.doi.org/10.1002/aic.12234.
[16] Aneggi E, Boaro M, De Leitenburg C, Dolcetti G, Trovarelli A. Insights into the redox properties of ceria-based oxides and their implications in catalysis. J Alloy Compd 2006;408–412:1096–102. http://dx.doi.org/10.1016/j.jallcom.2004.12.113.
[17] Bueno-López A, Krishna K, Makkee M, Moulijn J. Active oxygen from CeO_2 and its role in catalysed soot oxidation. Catal Lett 2005;99:203–5. http://dx.doi.org/10.1007/s10562-005-2120-x.
[18] Wu X, Liu S, Weng D, Lin F, Ran R. MnO_x-CeO_2-Al_2O_3 mixed oxides for soot oxidation: activity and thermal stability. J Hazard Mater 2011;187:283–90. http://dx.doi.org/10.1016/j.jhazmat.2011.01.010.
[19] Sun S, Chu W, Yang W. Ce-Al mixed oxide with high thermal stability for diesel soot combustion. Chin J Catal 2009;30:685–9. http://dx.doi.org/10.1016/S1872-2067(08)60118-7.
[20] Aneggi E, Wiater D, de Leitenburg C, Llorca J, Trovarelli A. Shape-dependent activity of ceria in soot combustion. ACS Catal 2014;4:172–81. http://dx.doi.org/10.1021/cs400850r.
[21] Bunluesin T, Putna ES, Gorte RJ. A comparison of CO oxidation on ceria-supported Pt, Pd, and Rh. Catal Lett 1996;41:1–5. http://dx.doi.org/10.1007/BF00811703.
[22] Park S, Vohs JM, Gorte RJ. Direct oxidation of hydrocarbons in a solid-oxide fuel cell. Nature 2000;404:265–7. http://dx.doi.org/10.1038/35005040.
[23] Yahiro H. Electrical properties and reducibilities of ceria-rare earth oxide systems and their application to solid oxide fuel cell. Solid State Ionics 1989;36:71–5. http://dx.doi.org/10.1016/0167-2738(89)90061-1.
[24] Adijanto L, Sampath A, Yu AS, Cargnello M, Fornasiero P, Gorte RJ, et al. Synthesis and stability of Pd@CeO_2 core-shell catalyst films in solid oxide fuel cell anodes. ACS Catal 2013;3:1801–9. http://dx.doi.org/10.1021/cs4004112.
[25] Aneggi E, de Leitenburg C, Trovarelli A. On the role of lattice/surface oxygen in ceria–zirconia catalysts for diesel soot combustion. Catal Today 2012;181:108–15. http://dx.doi.org/10.1016/j.cattod.2011.05.034.
[26] Reddy BM, Khan A. Nanosized CeO_2–SiO_2, CeO_2–TiO_2, and CeO_2–ZrO_2 mixed oxides: influence of supporting oxide on thermal stability and oxygen storage properties of ceria. Catal Surv Asia 2005;9:155–71. http://dx.doi.org/10.1007/s10563-005-7552-1.
[27] Atribak I, Bueno-López A, García-García A. Thermally stable ceria–zirconia catalysts for soot oxidation by O_2. Catal Commun 2008;9:250–5. http://dx.doi.org/10.1016/j.catcom.2007.05.047.
[28] Kwon HT, Mahamulkar S, Sulmonetti T, Min B, Malek A, Li L, et al. Sol-Gel Derived CeO_2/α-Al_2O_3 Bilayer Thin Film as an Anti-Coking Barrier and its Catalytic Coke Oxidation Performance, Manuscr. Prep. (n.d.).
[29] Damyanova S, Perez CA, Schmal M, Bueno JMC. Characterization of ceria-coated alumina carrier. Appl Catal A Gen 2002;234:271–82. http://dx.doi.org/10.1016/S0926-860X(02)00233-8.
[30] Martınez A, Ferna M, Conesa JC, Soria J. Structural and redox properties of ceria in alumina-supported ceria catalyst supports. J Phys Chem B 2000;104:4038–46.
[31] Shyu JZ, Weber WH, Gandhi HS. Surface characterization of alumina-supported ceria. J Phys Chem 1988;92:4964–70. http://dx.doi.org/10.1021/j100328a029.
[32] Bensalem A, Muller JC, Bozon-Verduraz F. From bulk CeO_2 to supported cerium-oxygen clusters: a diffuse reflectance approach. J Chem Soc, Faraday Trans 1992;88:153. http://dx.doi.org/10.1039/ft9928800153.
[33] Bueno-López A, Krishna K, Makkee M, Moulijn J. Enhanced soot oxidation by lattice oxygen via La^{3+}-doped CeO_2. J Catal 2005;230:237–48. http://dx.doi.org/10.1016/j.jcat.2004.11.027.
[34] Katta L, Sudarsanam P, Thrimurthulu G, Reddy BM. Doped nanosized ceria solid solutions for low temperature soot oxidation: zirconium versus lanthanum promoters. Appl Catal B Environ 2010;101:101–8. http://dx.doi.org/10.1016/j.apcatb.2010.09.012.
[35] Bueno-López A, Krishna K, van der Linden B, Mul G, Moulijn JA, Makkee M. On the mechanism of model diesel soot-O_2 reaction catalysed by Pt-containing La_{3+}-doped CeO_2 A TAP study with isotopic O_2. Catal Today 2007;121:237–45. http://dx.doi.org/10.1016/j.cattod.2006.06.048.
[36] Echevsky GV, Ayupov AB, Paukshtis EA, Coke deactivation of acid sites on ZSM-5 zeolite, Catal. Deactiv. 2001, Proc. 139 (2001) pp. 77–84. ISI: 000177817200010.
[37] Rostrup-Nielsen JR. Mechanisms of carbon formation on nickel-containing catalysts. J Catal 1977;48:155–65. http://dx.doi.org/10.1016/0021-9517(77)90087-2.
[38] Sadezky A, Muckenhuber H, Grothe H, Niessner R, Pöschl U. Raman microspectroscopy of soot and related carbonaceous materials: spectral analysis and structural information. Carbon 2005;43:1731–42. http://dx.doi.org/10.1016/j.carbon.2005.02.018.
[39] Ivleva NP, Messerer A, Yang X, Niessner R, Pöschl U. Raman microspectroscopic analysis of changes in the chemical structure and reactivity of soot in a diesel exhaust aftertreatment model system. Environ Sci Technol 2007;41:3702–7. http://dx.doi.org/10.1021/es0612448.
[40] Madier Y, Descorme C, Le Govic AM, Duprez D. Oxygen mobility in CeO_2 and $Ce_{(x)}Zr_{(1-x)}O_2$ compounds: study by CO transient oxidation and $^{18}O/^{16}O$ isotopic exchange. J Phys Chem B 1999;103:10999–1006. http://dx.doi.org/10.1021/jp991270a.
[41] Yin K, Mahamulkar S, Shibata H, Malek A, Jones CW, Agrawal PK, et al. Catalytic oxidation of solid carbon and carbon monoxide over cerium-zirconium mixed oxides. AIChE J 2017;63:725–38. http://dx.doi.org/10.1002/aic.15575.
[42] Gamarra D, Munuera G, Hungría AB, Fernández-García M, Conesa JC, Midgley PA, et al. Structure-activity relationship in nanostructured copper-ceria-based preferential CO oxidation catalysts. J Phys Chem C 2007;111:11026–38. http://dx.doi.org/10.1021/jp072243k.